

RESEARCH

Open Access



Analysis of secondary metabolites and morphology in *Streptomyces rimosus* microparticle-enhanced cultivation (MPEC) at various initial organic nitrogen concentrations

Anna Ścigaczewska^{1*} , Tomasz Boruta¹, Weronika Grzesiak¹ and Marcin Bizukojć¹

Abstract

The influence of talc microparticles on metabolism and morphology of *S. rimosus* at various initial organic nitrogen concentrations was investigated. The shake flask cultivations were conducted in the media with yeast extract (nitrogen source) concentration equal to 1 g YE L⁻¹ and 20 g YE L⁻¹. Two talc microparticle concentrations of 5 g TALC L⁻¹ and 10 g TALC L⁻¹ were tested in microparticle-enhanced cultivation (MPEC) runs. A high nitrogen concentration of 20 g YE L⁻¹ promoted the development of small agglomerates (pellets) of projected area lower than 10⁵ μm² and dispersed pseudohyphae. A low nitrogen concentration of 1 g YE L⁻¹ led to the limitation of *S. rimosus* growth and, in consequence, the development of the smaller number of large pseudohyphal agglomerates (pellets) of projected area higher than 10⁵ μm² compared to the culture containing a high amount of nitrogen source. In both cases talc microparticles were embedded into pellets and caused the decrease in their sizes. The lower amount of talc (5 g TALC L⁻¹) usually caused the weaker effect on *S. rimosus* morphology and metabolite production than the higher one. This correlation between the microparticles effect on morphology and metabolism of *S. rimosus* was especially noticeable in the biosynthesis of oxytetracycline, 2-acetyl-2-dicarboxamide oxytetracycline (ADOTC) and spinoxazine A. Compared to the control run, in MPEC their levels increased 4-fold, 5-fold and 1.6-fold respectively. The addition of talc also improved the production of 2-methylthio-cis-zeatin, lorneic acid J and milbemycin A₃.

Keywords Microparticle-enhanced cultivation, Morphological engineering, Organic nitrogen, *Streptomyces*, Secondary metabolites

*Correspondence:

Anna Ścigaczewska
anna.kowalska.1@p.lodz.pl

¹Faculty of Process and Environmental Engineering, Department of Bioprocess Engineering, Lodz University of Technology, ul. Wólczajska 213, Łódź 93-005, Poland



© The Author(s) 2024. **Open Access** This article is licensed under a Creative Commons Attribution-NonCommercial-NoDerivatives 4.0 International License, which permits any non-commercial use, sharing, distribution and reproduction in any medium or format, as long as you give appropriate credit to the original author(s) and the source, provide a link to the Creative Commons licence, and indicate if you modified the licensed material. You do not have permission under this licence to share adapted material derived from this article or parts of it. The images or other third party material in this article are included in the article's Creative Commons licence, unless indicated otherwise in a credit line to the material. If material is not included in the article's Creative Commons licence and your intended use is not permitted by statutory regulation or exceeds the permitted use, you will need to obtain permission directly from the copyright holder. To view a copy of this licence, visit <http://creativecommons.org/licenses/by-nc-nd/4.0/>.

Introduction

Actinomycetes are leading producers of many chemically and biologically active substances. One of the most recognisable microorganisms belonging to this group is *Streptomyces rimosus*, a producer of a wide spectrum of secondary metabolites, including oxytetracycline, an antibiotic from the tetracycline group [1, 2]. In order to biosynthesize chemical compounds by such filamentous microorganisms as *S. rimosus* it is necessary to adjust the level of the nutrients in the culture medium [3]. The two basic ingredients are carbon and nitrogen sources, and their presence in the cultivation medium is vital for the development of microorganisms and their metabolism.

Due to its importance, the issue of culture media composition in bioprocesses has been of constant interest. The most recent research on medium optimization in *Streptomyces* cultivations used statistical approach in the experiment design [4]. The authors used Plackett–Burman design (PBD) to find medium components that significantly affect the bioproduction of the secondary metabolite, valinomycin, by *Streptomyces* sp. ZJUT-IFE-354. Next they applied the central composite design (CCD) with Response Surface Methodology (RSM) to optimize the selected medium components. After the optimization procedure, the yield of valinomycin bioproduction increased 1.37-fold. The similar approach for *Streptomyces* can be found in the studies of Saleena et al. [5], Abdella et al. [6] and He et al. [7]. Preethi et al. [8] cultivated *Streptomyces coelicolor* SPR7 for peroxidase bioproduction using PBD and RSM method combined with artificial intelligence Back Propagation Algorithm (BPA) to optimize the process. Peroxidase amount increased 7-fold in comparison to the culture conducted with the non-optimized medium. Alloun et al. [9] obtained up to 4.5-fold enhancement of indole-3-acetic acid (IAA) bioproduction by *Streptomyces rubrogriseus* AW22 using RSM and introducing artificial neural networks (ANN) to the process optimization. What is noteworthy, in the case of secondary metabolites medium optimization does not mean keeping substrates on the level which results in the most effective microbial growth. Environmental stress in the microbial cultivation, which can be triggered by the insufficient amount of nutrients, was proven to be an effective way to force fungi and bacteria to change metabolite bioproduction in order to survive [10]. In the aforementioned works, however, *Streptomyces* morphological development was not studied and it is proven that not only does the metabolism of filamentous microorganisms depend on culture medium composition or generally process conditions, but it is also directly related to their morphology, either dispersed or pelleted [11]. On the other hand, changing the culture medium composition, especially the amount and type of carbon, nitrogen and phosphorus source, as

well as the concentration of oxygen or carbon dioxide, can significantly influence the developing morphological forms [12]. Unfortunately, when agglomerate (pellet) size increases above a certain critical value, the metabolic activity inside their core is limited due to the insufficient diffusion of oxygen and nutrients [13]. Therefore, in order to solve problems arising from the relationships between the availability of crucial substances, microbial morphology and their metabolism modern morphological engineering techniques have been developed [14]. To these methods belongs the microparticle-enhanced cultivation (MPEC). It allows for the change of the microorganism morphology and consequently metabolite formation without affecting the optimized composition of the medium [15–17]. Microparticle addition to filamentous fungi and actinomycete cultivations strongly influence on these microorganisms by physical interactions and gene regulation. *Streptomyces albus* J1074/R2 cultivated with talc microparticles developed pellets whose size was six-fold smaller in comparison to the control runs without the addition of the micromaterial [18]. These morphological changes were connected with the modifications of expression of 3341 genes, responsible both for growth and metabolism of the microorganism and it also resulted in three-fold enhancement of pama-mycin production to 50 mg L⁻¹ [18]. Talc addition in the cultivation of *Streptomyces lividans* led to analogous results [17]. In *S. lividans* MPEC pellets grew smaller (up to 40%) and changes in gene clusters and metabolite production were observed.

As the appropriate cultivation medium composition and the microbial morphology are the fundamental issues in every bioprocess involving filamentous microorganisms, there is a constant need for development in this field [19]. Recent studies have shown that industrial bioprocesses using *Streptomyces* are more efficient when the microorganism grows in a dispersed form [20]. Therefore, Kumar et al. [20] thoroughly investigated *Streptomyces toxytricini* mycelial evolution from spores to pellets using partial proteomic analysis and microscopic analysis. *Streptomyces* hyphae demonstrated the formation of septa, apical growth and branching behind the hyphae tip. Next, the branches of the hyphae agglomerated and probably formed cross-walls. Many proteins, especially DivIVA, were involved in these processes. Next, the branched hyphae of *Streptomyces toxytricini* agglomerated and further transformed into more compact morphological forms and, as a result, pellets were developed [20].

In the literature reports the positive effect of talc addition in MPEC was attributed to the decrease in the size of agglomerates (pellets) by preventing agglomeration of hyphae and physical destruction of the already developed agglomerates by increasing the shear forces caused

by microparticles [21]. The smaller agglomerates mean a shorter diffusion distance for nutrients and oxygen from the culture medium to the interior of the agglomerate, resulting in higher concentrations of secondary metabolites and enzymatic activities [21]. An example of linking the reduction of agglomerate size with the increase of the amount of bioproduct concentration is the work of Yue et al. [22]. They cultivated *Streptomyces gilvosporeus* Z8 with talc microparticles (diameter range of 6–45 μm). Natamycin titer in MPEC was 1.7-fold higher and the size of the pellets decreased even 10-fold compared to the cultivations without talc. A similar effect was observed in *Streptomyces toxytricini* KD18 cultivation [23]. The addition of glass beads and silica particles to the culture medium increased lipstatin production 4-fold, and caused to the formation of smaller pellets and dispersed pseudomycelia.

Nevertheless, there is a limited number of studies reporting *Streptomyces* morphology in detail with the use of morphological parameters and there are no studies linking the influence of culture medium composition with MPEC and formation of secondary metabolites at all. This work fills this gap by performing the *Streptomyces rimosus* cultivations with talc microparticle addition at various initial organic nitrogen concentrations.

Materials and methods

Cultivated microorganism

The actinomycete *Streptomyces rimosus* ATCC 10970 stored on medium Difco™ ISP2 agar slants was used in the study. To induce *S. rimosus* sporulation, 5 days before the experiments its spores were inoculated onto freshly prepared agar slants and incubated at 26 °C.

Medium composition

In order to investigate the influence of talc microparticles on the metabolism and morphology of *S. rimosus* at two various nitrogen contents, the microorganism cultivations were carried out in shake flasks of 150 ml working volume on the media differing by the concentration of

yeast extract being the sole nitrogen source. Moreover, these cultivations were carried out simultaneously in the runs with the addition of 10 μm talc microparticles (MPEC) and without it (control). The following concentrations of yeast extract (YE) were used: 1 g YE L⁻¹ and 20 g YE L⁻¹. The concentrations of the added talc microparticles (TALC) were 5 g TALC L⁻¹ and 10 g TALC L⁻¹. The amounts of the other substances in the medium were identical for each run of the experiment: glucose (20 g L⁻¹), KH₂PO₄ (1.50 g L⁻¹), MgSO₄·7H₂O (0.52 g L⁻¹), NaCl (0.4 g L⁻¹), ZnSO₄·7H₂O (1 mg L⁻¹), Fe(NO₃)₃·9H₂O (2 mg L⁻¹), biotin (0.04 mg L⁻¹), H₃BO₃·7H₂O (0.065 mg L⁻¹), MnSO₄·7H₂O (0.07 mg L⁻¹), CuSO₄·5H₂O (0.25 mg L⁻¹), Na₂MoO₄·2H₂O (0.05 mg L⁻¹).

The talc microparticle powder 3MgO·4SiO₂·H₂O used in the study was produced by Thermo Scientific (USA) intended for research and development with molecular weight 379.28, particle size–350 mesh (mean diameter 10 μm , diameter range of 6–45 μm), density 2.7 g cm⁻³ at 20 °C, CAS number 14807-96-6.

The conducted study was divided into two experiments with each of them consisting of four runs (Table 1).

Both experiments were performed in triplicate in a Certomat® BS-1 shaker (B. Braun Biotech International, Berlin, Germany) at the temperature of 28 °C and rotational speed 110 rpm. The cultivation time was 96 h. Samples were collected and analysed every 24 h

Inoculation procedure

For one run of experiment 1 slant of *S. rimosus* and 5 shake flasks (1 flask for each of the 5 days of the experiment) were prepared. To standardize the inoculum within an individual experiment consisting of four runs, four slants were washed under sterile conditions into 700 ml of physiological saline and mixed. A 30 ml of inoculum was next poured into each previously prepared flasks containing 100 ml of concentrated culture medium. The flasks were then refilled with 20 ml of saline with microparticles of talc (MPEC) or pure saline solution (control). As a result, 20 shake flasks containing 150 ml of the medium in four runs were inoculated from one inoculum. All substrates and tools used were autoclaved for 30 min at 121 °C.

Analytical methods

Image analysis

The samples of the culture broth for the morphological analysis of *S. rimosus* were collected every 24 h and observed with an optical phase contrast microscope (OLYMPUS BX53, Olympus Corporation, Japan). In the next step, high-resolution RGB digital camera (OLYMPUS DP27) was used to take the microscopic images of the observed morphological objects and image analysis

Table 1 Runs conducted in experiments 1 and 2 with their abbreviations

| | Abbreviation | Yeast extract concentration (g YE L ⁻¹) | Talc concentration (g TALC L ⁻¹) |
|--------------|--------------|---|--|
| Experiment 1 | YE1TALC0_1 | 1 | 0 |
| | YE1TALC10_1 | 1 | 10 |
| | YE20TALC0_1 | 20 | 0 |
| | YE20TALC10_1 | 20 | 10 |
| Experiment 2 | YE1TALC0_2 | 1 | 0 |
| | YE1TALC5_2 | 1 | 5 |
| | YE20TALC0_2 | 20 | 0 |
| | YE20TALC5_2 | 20 | 5 |

software (OLYMPUS cellSens Dimension Desktop 1.16, Olympus Corporation, Japan) was used for digital image analysis. After applying Sobel, median and size filters three morphological parameters were calculated: projected area (A), elongation (E) and morphology number (Mo). Projected area determines the size of the morphological objects and elongation describes their shape. Morphology number Mo was defined by Wucherpfennig et al. [24] and combines size and shape morphological parameters.

$$Mo = \frac{2 \cdot \sqrt{A} \cdot S}{\sqrt{\pi} \cdot D \cdot E}$$

OLYMPUS cellSens Dimension Desktop 1.16 determines all these morphological parameters as follows: “A - projected area, the number of pixels contained in an object multiplied by the squared calibration unit; E - elongation, the squared quotient of longitudinal and transversal deviation of all pixels belonging to the object along the regression, S - solidity (also known as roughness R), the area relative to the area of the object’s convex hull line, D - maximum diameter of the object”. The detailed description of all these morphological parameters can be found in [25].

Chemical analyses

The secondary metabolites identification was conducted in the positive ESI+ and the negative ESI- electrospray ionization modes of high-resolution mass spectrometry (ACQUITY-SYNAPT G2, Waters, USA. TargetLynx software (Waters, USA). The oxytetracycline standard and the Natural Products Atlas database of metabolites [<https://www.npatlas.org/>] were used for the quantitative and semi-quantitative analyses of the secondary metabolites. A detailed description of the procedure was provided by Boruta et al. [26]. The calibration for UPLC-MS analysis was performed with the use of 5 mM sodium formate solution in 90:10 (v/v) 2-propanol/water. The solution of leucine enkephalin (C₂₈H₃₇N₅O₇) at the concentration of 2 ng μl⁻¹ was used as the lock-mass in the accurate measurements of the mass of ions throughout the study.

Glucose concentration was assayed with the use of ultra-high performance liquid chromatography (UPLC® Acquity, Waters, USA) on a UPLC BEH Amide column (2.1 mm × 150 mm × 1.7 μm, Waters, USA) with the use of evaporated light scatter detector (ELSD). The analysis temperature was 35 °C. Eluent contained 75% acetonitrile deionized water solution with 0.2% of triethylamine and its flow rate was 0.29 ml min⁻¹.

Samples were harvested every 24 h of the cultivations, filtered with the use of paper filters (density 84 g m⁻³) to remove biomass and microparticles and stored at a

temperature of -18 °C. Samples intended for the chemical analyses were thawed at room temperature prior to analysis and filtered with the use of 0.2 μm syringe filters.

Calculations and statistical analysis

The effect of microparticles on the metabolism was described in the form of Enhancement Factor (EF) [16]. This parameter is calculated as the concentration or level of a metabolite obtained in the cultivation with talc (MPEC) divided by the concentration or level of this metabolite in the control run (without talc added). If it is equal to 1, it means there is no effect. The values higher than 1 indicates the positive effect of microparticles while those below 1 on the negative one. Standard deviations for EF were calculated on the basis of the statistical analysis for the concentration or level of a metabolite in the control run and MPEC run according to the formula:

$$\frac{\Delta EF}{EF} = \frac{\Delta A}{A} + \frac{\Delta B}{B}$$

where: A - concentration or level of a metabolite in the control run (without talc added), ΔA - standard deviation for A, B - concentration or level of a metabolite in MPEC, ΔB - standard deviation for B, EF - enhancement factor and ΔEF - standard deviation for EF.

In order to obtain reliable data, each experiment was performed in triplicate. Significance level α was set at 0.05. Statistical t-test was used for P-values calculations. Standard deviations were calculated for the mean values of the glucose and metabolite concentrations. Morphological parameters were calculated as mean values obtained from samples containing up to 8000 objects. The smallest tested set of objects was not smaller than 30 objects, which allowed for obtaining statistically significant results and the possibility of calculating confidence intervals.

Results

Effect of nitrogen source amount and talc microparticles on *S. rimosus* morphology

During the preliminary visual analysis of *S. rimosus* morphology the pseudomycelial objects of *S. rimosus* were divided into two classes. The first class (hereafter referred to as the class of agglomerates) consisted of round regular pellets, irregular pellets and clump forms. The second class (referred to as the class of non-agglomerates) contained the non-agglomerated morphological objects, mainly free pseudohyphae both branched and unbranched or circular spores. The exemplary microscopic images of *S. rimosus* morphological forms are presented in Fig. 1.

The morphological objects obtained in 24 h of YE1T-ALC0_1 run were the examples of pellets with the

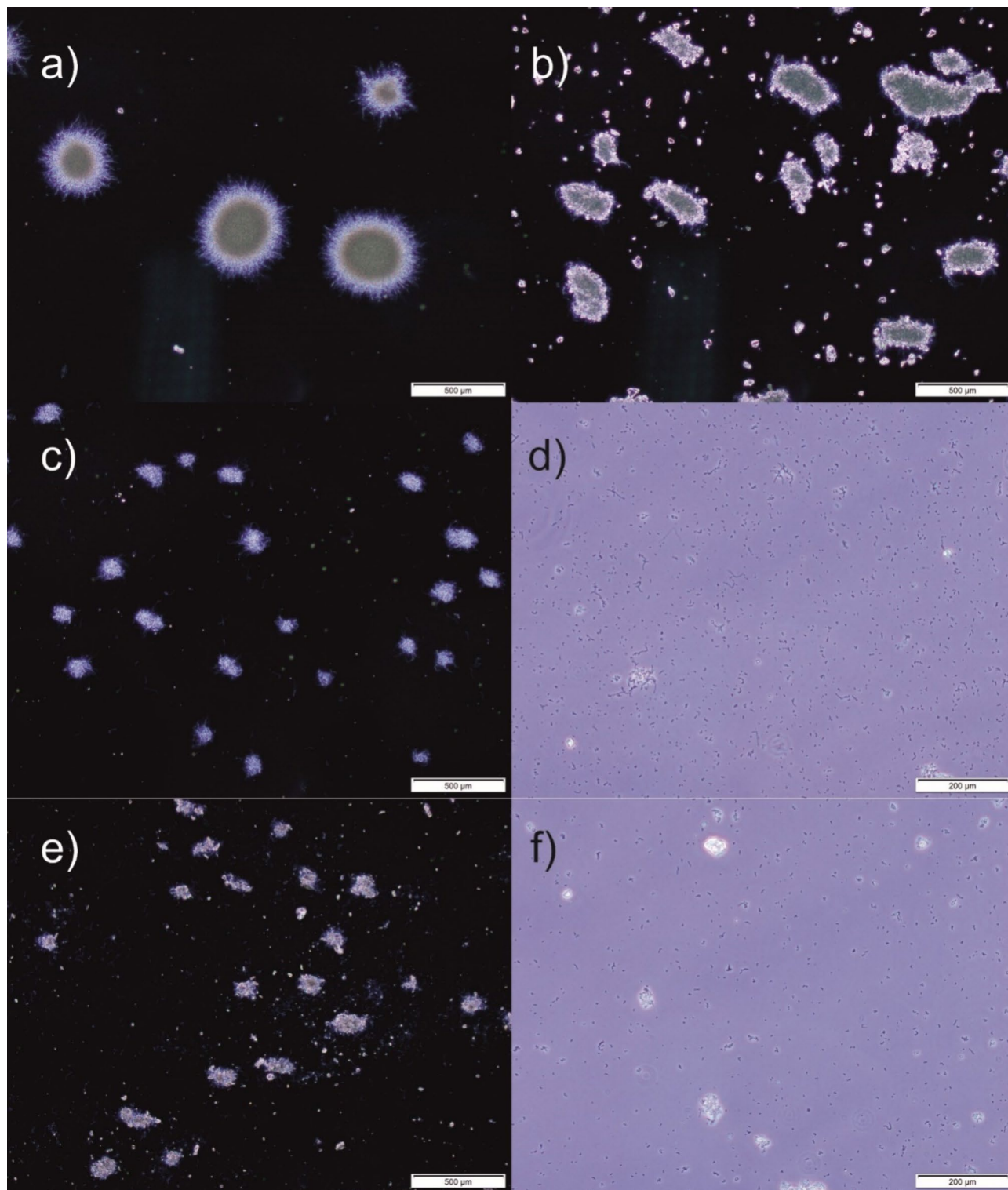


Fig. 1 The exemplary microscopic images of: **(a)** circular pellets developed in the run YE1TALC0_1 without microparticles addition and 1 g YE L^{-1} ; **(b)** irregular pellets with embedded talc microparticles developed in the run YE1TALC10_1 with 10 g TALC L^{-1} and 1 g YE L^{-1} ; **(c)** irregular pellets developed in the run YE20TALC0_1 without microparticles and 20 g YE L^{-1} ; **(d)** dispersed pseudomycelium developed in the run YE20TALC0_1 without microparticles and 20 g YE L^{-1} ; **(e)** irregular pellets with embedded talc microparticles developed in the run YE20TALC10_1 with 10 g TALC L^{-1} and 20 g YE L^{-1} ; **(f)** dispersed pseudomycelium developed in the run YE20TALC10_1 with 10 g TALC L^{-1} and 20 g YE L^{-1} . Pellets images were snapped in 24 h of the runs; dispersed pseudomycelium images were snapped in 96 h of the runs

characteristic distinct cores (Fig. 1a). They developed in the medium without talc microparticles. Figure 1b also shows pellets after 24 h of the experiment, but for the YE1TALC10_1 run, in which talc particles were embedded in the structure of the pellets and consequently changed their shapes. Figure 1c and d show the morphological objects formed by *S. rimosus* in 24 h of YE20TALC0_1 run. Agglomerated (class of agglomerates) and non-agglomerated (class of non-agglomerates) objects are shown in the separate images (Fig. 1c and d). In the case of the class of agglomerates (Fig. 1c) one can distinguish both pellets and clumps that do not have a regular, compact structure. The class of non-agglomerates that included non-agglomerated elongated pseudohyphae (branched and unbranched) and very small, spherical spores is exemplified in Fig. 1d. The last two images (Fig. 1e and f) present both classes of *S. rimosus* morphological objects in 24 h of YE20TALC10_1 run. Comparing the runs YE20TALC0_1 and YE20TALC10_1, the addition of talc to the latter one led to the development of pellets with more compact structure and embedded microparticles (Fig. 1e). In the case of the class of non-agglomerates from YE20TALC10_1 (Fig. 1f) pseudohyphae were not visibly different from the corresponding objects raised without talc addition in YE20TALC0 run (Fig. 1d). In the experiment 2 with talc addition at the concentration of 5 g L⁻¹ (YE1TALC0_2, YE1TALC5_2, YE20TALC0_2, YE20TALC5_2, pictures not shown) morphological objects of *S. rimosus* developed in the same way as in the experiment 1 (YE1TALC0_1, YE1TALC10_1, YE20TALC0_1, YE20TALC10_1, Fig. 1). However, the lower amount of talc caused the weaker effect on *S. rimosus* morphology, which is seen upon the values of morphological parameters (Figs. 2, 3 and 4).

Comparing the effect of nitrogen source, the low concentration of yeast extract (1 g YE L⁻¹) in the runs YE1TALC0_1, YE1TALC10_1 led to the limitation of *S. rimosus* growth and, in consequence, the development of the smaller number of large pseudohyphal agglomerates (Fig. 1a and b) than in the culture containing higher amount of nitrogen source (Fig. 1c-f). The high concentration of yeast extract in the runs YE20TALC0_1, YE20TALC10_1 (20 g L⁻¹) promoted the development of small agglomerates and dispersed pseudohyphae (Fig. 1c-f). Predictably, the same effect of nitrogen source on *S. rimosus* morphology was observed in the second experiment (YE1TALC0_2, YE1TALC5_2, YE20TALC0_2, YE20TALC5_2, pictures not shown).

Figure 2 shows the changes of the values of projected area, morphology number and elongation for both classes of objects (agglomerates and non-agglomerates) from experiment 1 (10 g TALC L⁻¹). In the first 24 h, the rapid growth of the microorganism was observed (Fig. 2a). Projected area of the class of agglomerates increased

from 1.0·10³ to 2.0·10⁵ μm². As expected, the objects in the class of non-agglomerates were significantly smaller with the highest value of projected area equal to 1.0·10² μm². What is more, this class was present only in the runs with 20 g YE L⁻¹ in the culture medium (YE20TALC0_1, YE20TALC10_1) and it could be definitely attributed to the nitrogen-rich conditions in this run. In the runs conducted in the medium containing 1 g YE L⁻¹ (YE1TALC0_1, YE1TALC10_1) most of the hyphae agglomerated independent of the presence of talc microparticles, forming pellets belonging to the class of the agglomerates (Fig. 2a).

Morphology number (Fig. 2b) at the beginning of the experiment 1 (0 h) was 0.7. This value describes the morphology of circular spores that were present at this moment of the cultivations. During the first 24 h of the runs YE20TALC0_1 and YE20TALC10_1 morphology number of non-agglomerated objects decreased below 0.20 due to the hyphal growth. In 48 h *S. rimosus* agglomerated leaving only non-elongated objects in the class of non-agglomerates, which caused to the increase of morphology number up to the value of 0.40. This value was maintained until the end of the experiment.

The course of elongation changes in all runs of experiment 1 (Fig. 2c) was correlated with morphology number. In 0 h elongation calculated for circular spores was relatively low at the level of 1.16. As the filaments were becoming longer, elongation of the non-agglomerated objects in the class of non-agglomerates increased even to 4.32 in 24 h (YE20TALC0). Afterwards, in 48 h this value decreased and maintained in the range from 1.65 to 1.90 until the end of the experiment. Because of the irregular shapes of the agglomerates in the runs YE1TALC10_1, YE20TALC0_1, YE20TALC10_1 (Fig. 1) their morphology number and elongation had similar values to those for the objects from the non-agglomerated class (Fig. 2b and c). In the experiment YE1TALC0_1, in which distinct and circular pellets developed (Fig. 1a), their morphology number was significantly higher in comparison to the other runs of experiment 1 (Fig. 2b) and corresponding elongation did not exceed 1.50 (Fig. 2c).

The time course of the morphological parameters only for the class of agglomerates, that developed in experiment 1, is presented in Fig. 3. The highest projected area was obtained for *S. rimosus* agglomerates in YE1TALC0_1 run (Fig. 3a). Projected area of pellets in 24 h was equal to 2.0·10⁵ μm². In the corresponding run of experiment 1 with talc addition, YE1TALC10_1, the pellets were markedly lower. The projected area of the pellets in 24 h in YE1TALC10_1 was equal to 5.7·10⁴ μm². The difference between these two values was statistically significant with $p < 0.0001$. Therefore, in these runs of experiment 1 talc addition influenced the size of the agglomerates leading to the development of smaller

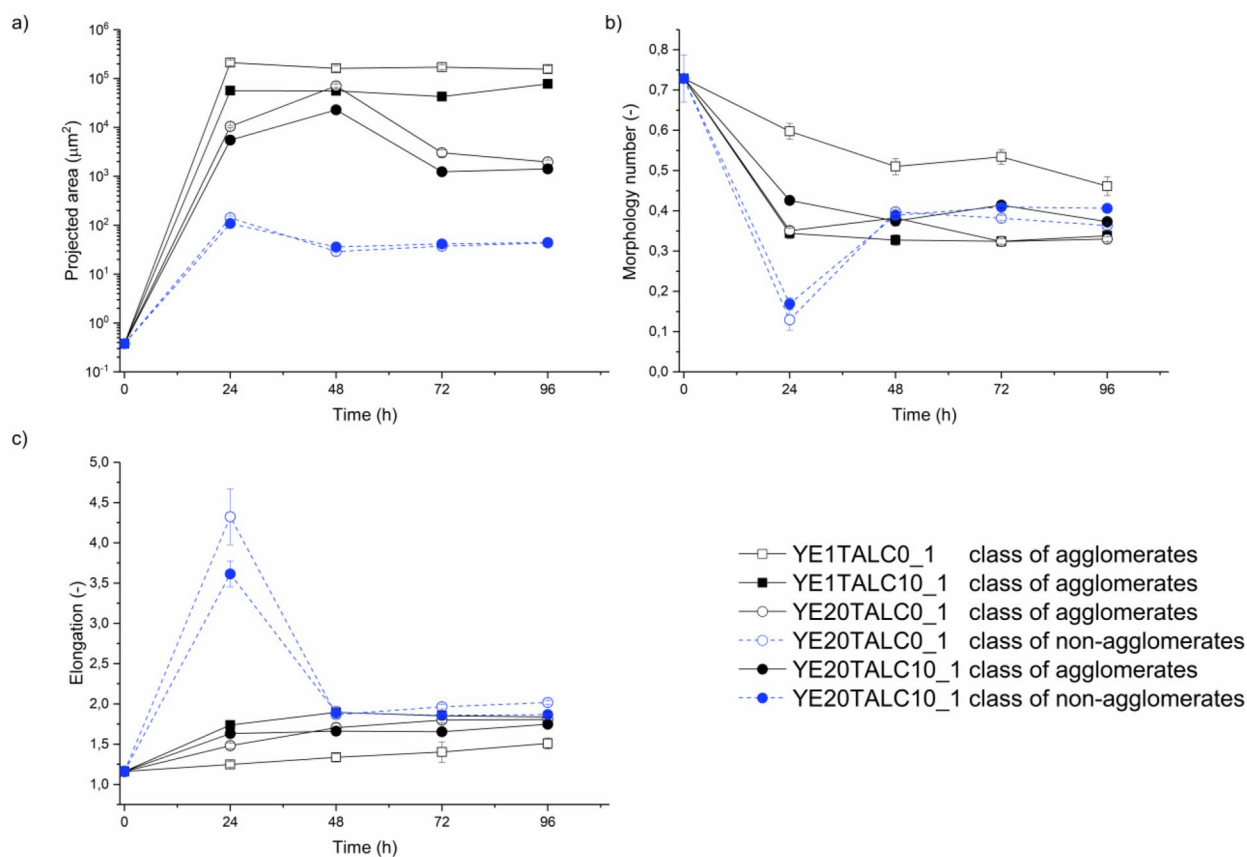


Fig. 2 Projected area (a), morphology number (b) and elongation (c) for agglomerates and non-agglomerated objects from experiment 1 (10 g TALC L⁻¹)

morphological objects. The similar dependence was observed in YE20TALC0_1 and YE20TALC10_1 (Fig. 3a). The largest agglomerates in these two runs were observed in 48 h and their corresponding projected area values were equal to $7.1 \cdot 10^4 \mu\text{m}^2$ for YE20TALC0_1 and $2.3 \cdot 10^4 \mu\text{m}^2$ for YE20TALC10_1 ($p < 0.0001$).

Apart from talc addition, yeast extract concentration was the factor influencing *S. rimosus* morphology too. Limited nitrogen source in YE1TALC0_1 run contributed to the growth of circular pellets with a distinct core (Fig. 1a) and of larger size (Fig. 3a) in comparison to the agglomerates from the other runs of experiment 1. The time changes of the projected area in the runs with 1 g YE L⁻¹ were different from those observed in the runs with yeast extract concentration equal to 20 g YE L⁻¹ (Fig. 3a). In YE1TALC0_1 and YE1TALC10_1 runs the phase of intensive pseudomycelial growth lasted 24 h, while in YE20TALC0_1 and YE20TALC10_1 runs the agglomerates were growing until 48 h. In the next hours of the runs with 20 g YE L⁻¹ the decrease in the size of pseudomycelial objects occurred, which did not take place in YE1TALC0_1 and YE1TALC10_1 runs.

Another morphological parameter shown in Fig. 3 is morphology number of the agglomerates from the

experiment 1 (Fig. 3b). Only in the case of YE1TALC0_1 run morphology number value did not decrease below 0.50 since the beginning of the experiment. Its exact value in 24 h was equal to 0.61 and indicated the formation of circular and regular objects. The corresponding value of elongation (Fig. 2c) reached 1.25 which confirmed the direct observations of the circular shape of the agglomerates. In the other runs of experiment 1 (YE1TALC10_1, YE20TALC0_1, YE20TALC10_1) morphology number for the agglomerates ranged from 0.45 to 0.32 due to their shapeless irregular forms (Figs. 1 and 3b). Noteworthy is the fact that talc addition influenced the time changes of elongation in the runs of the experiment 1 with both yeast extract concentrations (1 g YE L⁻¹ and 20 g YE L⁻¹, Fig. 3c). In YE1TALC0_1 and YE20TALC0_1 runs elongation was gradually increasing from the beginning of the experiment until 72 h. In YE1TALC10_1 and YE20TALC10_1 runs the rapid increase of this parameter was observed during the first 24 h only. The most elongated agglomerates were developed in YE1TALC10_1 run with elongation equal to 1.90 in 48 h.

Experiment 2 (Fig. 4) included the following runs: YE1TALC0_2, YE1TALC5_2, YE20TALC0_2, YE20TALC5_2. It differed from experiment 1 by lower talc

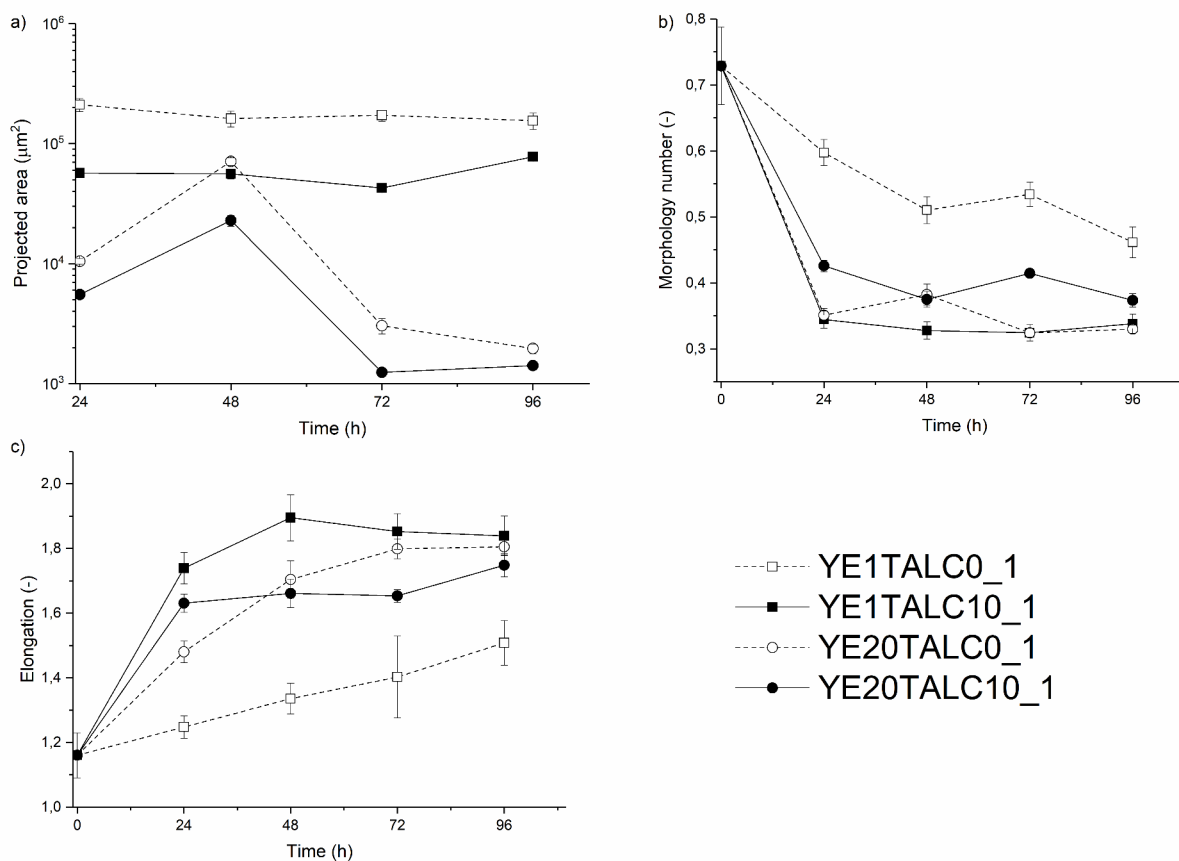


Fig. 3 Projected area (a), morphology number (b) and elongation (c) for the class of agglomerates developed in experiment 1 (10 g TALC L^{-1})

concentration added at the level of 5 g TALC L^{-1} . The decrease in the amount of talc microparticles (to see whether their effect on actinomycete morphology was still observable) seemed tempting from the practical point of view as the lower amount of raw material could be used. The medium composition used in the corresponding runs of both experiments was identical. The changes of morphological parameters for the class of agglomerates and non-agglomerates in the experiment 2 (Fig. 4) were similar to the ones from experiment 1 (Fig. 2). However, the values of the morphological parameters described below showed that the lower concentration of talc microparticles used in the experiment 2 led to the smaller differences between the values morphological parameters in the control and MPEC runs in comparison to experiment 1. The largest agglomerates developed in the runs with the lowest yeast extract concentration YE1TALC0_2 and YE1TALC5_2 (Fig. 4a). In 24 h their projected areas were equal to $1.3 \cdot 10^5 \mu\text{m}^2$ and $6.6 \cdot 10^4 \mu\text{m}^2$ respectively ($p < 0.0001$) and differed significantly what indicated on the effect of the microparticles despite their lower concentration. In comparison, the highest projected area in runs with 20 g YE L^{-1} in the culture

medium was obtained at 48 h. Their exact values were $3.9 \cdot 10^4 \mu\text{m}^2$ in YE20TALC0_2 and $3.5 \cdot 10^4 \mu\text{m}^2$ in YE20TALC5_2 ($p < 0.0001$).

The other morphological parameters calculated for the objects observed in experiment 2, morphology number (Fig. 4b) and elongation (Fig. 4c) were compliant with the direct observations. For the largest and the most circular pellets in YE1TALC0_2 run morphology number was the highest and did not decrease below 0.50. In the other runs of experiment 2 (YE1TALC5_2, YE20TALC0_2, YE20TALC5_2) both agglomerated and non-agglomerated objects were irregular, therefore morphology number was in the range from 0.20 to 0.45. Likewise, elongation (Fig. 4c) for the most circular agglomerates in YE1TALC0 was the lowest in comparison to the other runs, in which both agglomerated and non-agglomerated objects were more elongated (YE1TALC5_2, YE20TALC0_2, YE20TALC5_2). In 24 h the value of elongation was equal to 1.27 for the class of agglomerates in YE1TALC0_2. The corresponding value from YE1TALC5_2 reached 1.70, thus talc addition led to the increase of elongation. The values of agglomerate elongation in YE20TALC0_2 and YE20TALC5_2 runs were almost equal reaching 1.58 and

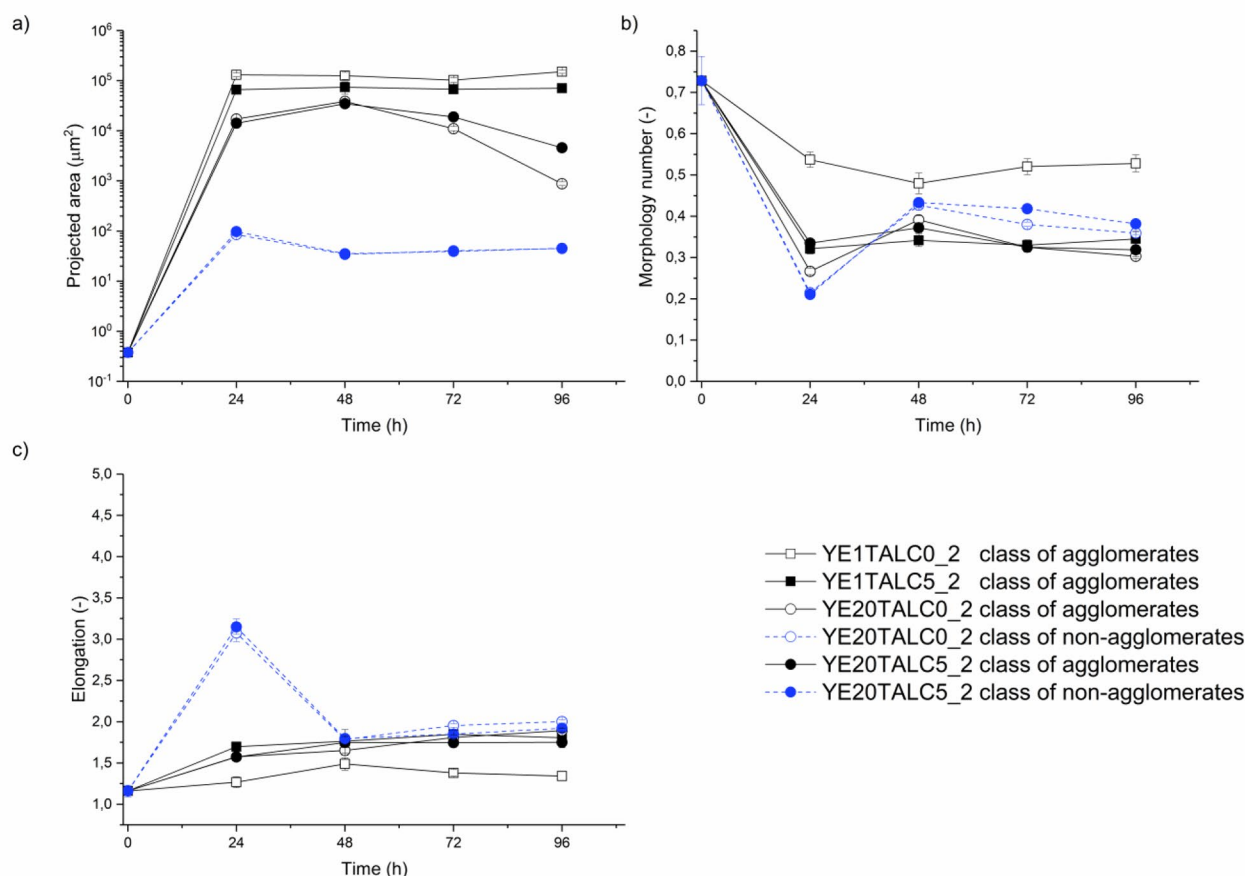


Fig. 4 Projected area (a), morphology number (b) and elongation (c) for agglomerates and non-agglomerated objects from the experiment 2 (5 g TALC L⁻¹)

1.57, respectively. The highest elongation was obtained for the non-agglomerated objects in YE20TALC0_2 and YE20TALC5_2. In 24 h of these two runs this parameter exceeded 3.00. In the experiment 1 the most elongated hyphae were also observed in 24 h of the runs with YE20 (YE20TALC0_2 and YE20TALC10_2 (Fig. 2).

Analysis of secondary metabolites

The analysis of *S. rimosus* secondary metabolite repertoire was based upon the ones detected by mass spectrometry and, if possible, identified upon the available databases. Eight secondary metabolites that gave the most marked signals were selected and they are presented in Fig. 5. For the sake of clarity, each run of the experiment corresponded to a different colour: YE20TALC10_1 red, YE20TALC5_2 yellow, YE1TALC10_1 green and YE1TALC5_2 blue. Secondary metabolite levels were defined with the use of the enhancement factor EF (see [Materials and methods](#) section) which is the common way to present the results on the effect of microparticles on microbial metabolism. With regard to the amount of nitrogen source used the detected pool of metabolites can be divided into those that are produced

under nitrogen-limited conditions only (1 g YE L⁻¹, e.g. oxytetracycline and ADOTC), in the nitrogen-rich condition only (e.g. 2-methylthio-cis-zeatin), and those occurring in both variants of nitrogen amount (e.g. lorneic acid J, milbemycin A₃, spinoxazine A).

The enhancement factor (EF) values obtained for oxytetracycline (Fig. 5a) in the YE1TALC10_1 run were markedly higher than 1. Therefore, talc addition enhanced oxytetracycline production. For the 72 h of the YE1TALC10_1 run EF was in the range from 2.5 to 4.0. In the run with the lower concentration of talc, YE1TALC5_2, the difference between MPEC and control was not significant ($p > 0.05$) (Fig. 5a).

ADOTC enhancement factors EF, presented in Fig. 5b, reached 5.0 in 48 h of YE1TALC10_1 run and 3.0 in 48 h in YE1TALC5_2 run. In the following hours of the experiments EF of ADOTC decreased systematically. Figure 5a and b show the same dependence for two studied compounds belonging to tetracycline group namely oxytetracycline and its derivative ADOTC. In the runs with 10 g TALC L⁻¹ their EFs were higher compared to the runs with 5 g TALC L⁻¹. For oxytetracycline, EF in the 72 h and 96 h of YE1TALC5_2 did not reach 1 which means

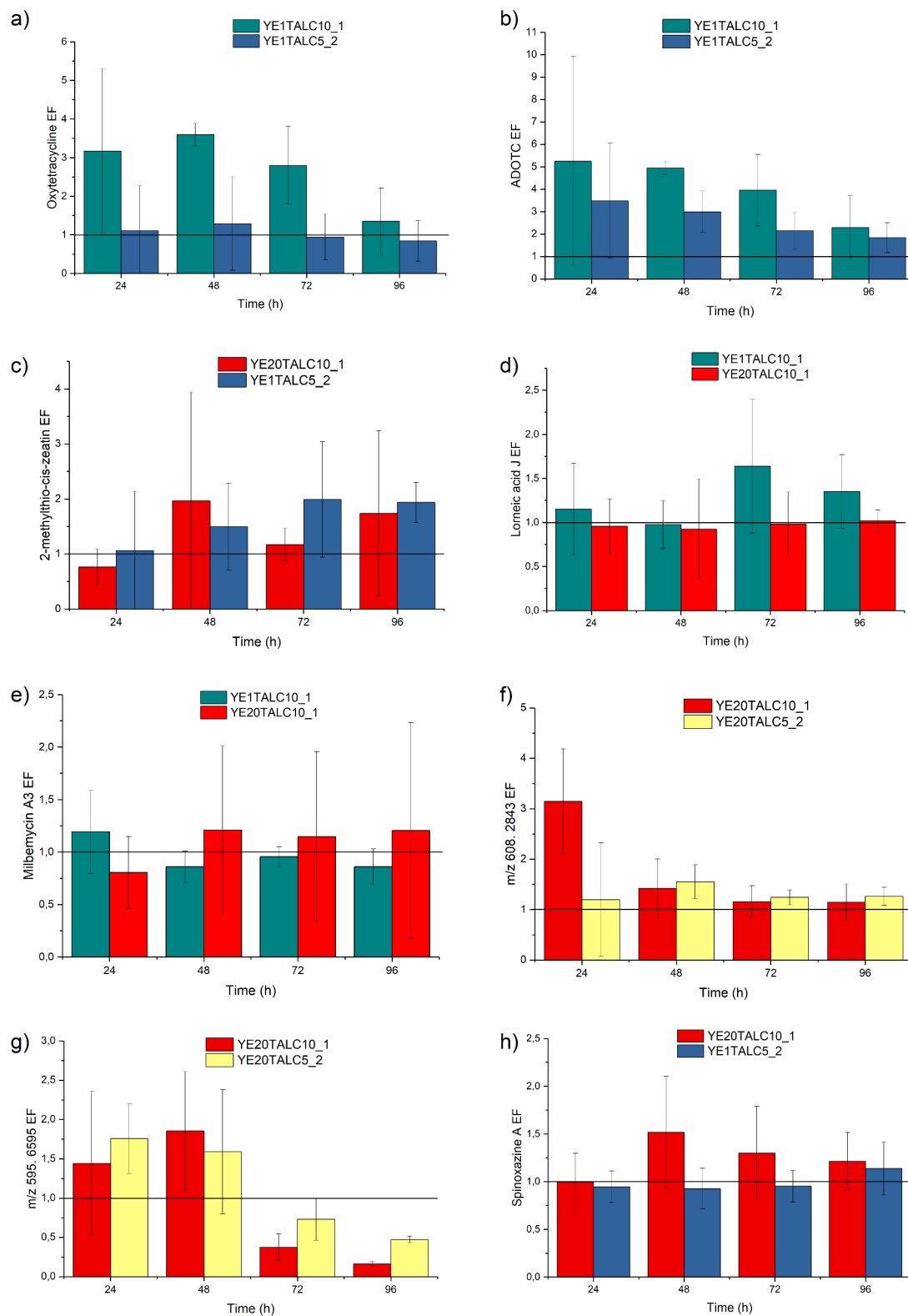


Fig. 5 Selected secondary metabolites enhancement factors EF. The more the FE value exceeds 1, the stronger the enhancing effect of microparticles on metabolite levels. EF calculations and statistical analysis methods are described in Sect. 2.4.3

that in this variant of MPEC the amount of the metabolite was lower than in control run.

At the beginning of the experiments EF for 2-methylthio-cis-zeatin (Fig. 5c) was close to 1 which indicated that the metabolite was hardly enhanced by talc addition. In 24 h exact EF values were equal to 1.1 in YE20TALC10_1 and 0.8 in YE1TALC5_2. The positive effect of talc addition on 2-methylthio-cis-zeatin bioproduction occurred after 48 h of the experiments. At the end of the experiments, EF for this metabolite reached 1.7 in YE20TALC10_1 and 1.9 in YE1TALC5_2.

Lorneic acid J EF values higher than 1 were obtained only in one out of the four conducted runs, YE1TALC10_1 (Fig. 5d). The highest lorneic acid J EF value in this run was equal to 1.6 in 72 h. The second run presented in Fig. 5d, YE20TALC10_1, was chosen to show the differences in EF levels caused by the change of yeast extract concentration. In the case of this particular metabolite, 10 g TALC L⁻¹ in the medium containing 1 g YE L⁻¹ (YE1TALC10_1) improved lorneic acid J production, whilst in the medium with 20 g YE L⁻¹ (YE20TALC10_1) the effect of talc addition was opposite and EF decreased below 1.

Figure 5e shows enhancement factor EF for milbemycin A₃ obtained in two runs of the experiments differing only by yeast extract concentration. Similar to lorneic acid J, this amount of nitrogen source in the culture medium influenced milbemycin A₃ EF. Importantly, for milbemycin A₃ the increase of EF to 1.2 was observed in MPEC with 20 g YE L⁻¹ (YE20TALC10_1 96 h), whereas in YE1TALC10_1 this EF decreased to 0.8 in 96 h. The example of lorneic acid J and milbemycin A₃ shows that the final effect of MPEC is also connected with medium composition.

Unidentified compounds with experimental *m/z* value [M-H]⁻ ion: *m/z*=608.2843 (Fig. 5f) and *m/z*=595.6595 (Fig. 5g) both showed high enhancement factors in 24 h and 48 h of the experiment 1. The highest EF values were equal to 3.1 for *m/z*=608.2843 (YE20TALC10_1 at 24 h) and 1.9 for *m/z*=595.6595 (YE20TALC10_1 at 48 h). Therefore, it can be concluded that for these compounds talc addition in MPEC caused the highest enhancement in bioproduction during the cultivations conducted on a medium containing 20 g YE L⁻¹. Enhancement factors EF for *m/z*=608.2843 and *m/z*=595.6595 obtained in the runs with 1 g YE L⁻¹, YE1TALC10_1 and YE1TALC5_2 (data not shown), were lower than 1.

In Fig. 5h, the positive influence of talc addition on spinoxazine A bioproduction by *S. rimosus* is shown. In 48 h of YE20TALC10_1 run EF achieved the highest value equal to 1.6. The higher concentration of spinoxazine A in MPEC compared to the control run also took place at lower talc concentration. In 96 h of YE1TALC5_2 EF for this compound was equal to 1.2.

Glucose utilization profiles

The profiles of glucose utilization by *S. rimosus* (Fig. 6) were strongly influenced by the initial concentration of yeast extract, being the nitrogen source. It is clearly seen that glucose concentration (GLU) decreased only by 3 to 4 g GLU L⁻¹ from the initial 20 g GLU L⁻¹ in the runs with the use of the media with 1 g YE L⁻¹. In the runs containing 20 g YE L⁻¹ glucose utilization reached 13 g GLU L⁻¹ within the process. These observations confirmed the expected growth limitation of *S. rimosus* caused by low nitrogen concentration (1 g YE L⁻¹). In the runs in which nitrogen was not the limiting factor (20 g YE L⁻¹), glucose was rapidly consumed. Interestingly, talc addition slightly improved glucose utilization by *S. rimosus* in the runs in which its pseudomycelial growth was nitrogen-limited (YE1TALC10_1 and YE1TALC5_2) in comparison to the control runs. In YE20TALC10_1 and YE20TALC5_2, in which nitrogen limitation was not the case, talc addition caused the opposite effect. Comparing these two runs to their control runs, lower glucose concentrations at the end of the run were observed in the runs without talc.

Discussion

The conducted research supplied new data on the morphological changes of *S. rimosus* and its effect on the secondary metabolism in the microparticle-enhanced cultivations (MPEC) in the media with various nitrogen source and talc microparticle concentrations. The influence of nutritional components and microbial morphology on the metabolism has been proven and is a well-known fact for other species [4, 19, 27, 28].

Analyzing *S. rimosus* mycelial development with the use of the morphological parameters, it can be concluded that under the same process conditions, both MPEC and control runs can generate different morphological forms dependent on the culture medium composition. In the conducted experiments, the largest pellets with the most regular shapes were obtained in the runs with 1 g YE L⁻¹ (Figs. 1a and 3a). The low concentration of nitrogen led to biomass growth limitation, confirmed by glucose utilization profiles (Fig. 6). According to the literature for the filamentous microorganisms, the amount of biomass is strongly associated with the diameter of developing pellets [29]. Considering physical interactions, a small number of mycelial (or pseudomycelial) objects present in the culture unable the interactions between mycelial objects and leaves space for their growth. This leads to the development of less number of larger agglomerates than in the culture containing a higher concentration of biomass (Figs. 1c and d and 3a). The high amount of yeast extract (20 g YE L⁻¹) allowed *S. rimosus* for the nitrogen unlimited growth. Bizukojć et al. (2023) [30] examined *S. rimosus* cultivated in the media with various concentrations

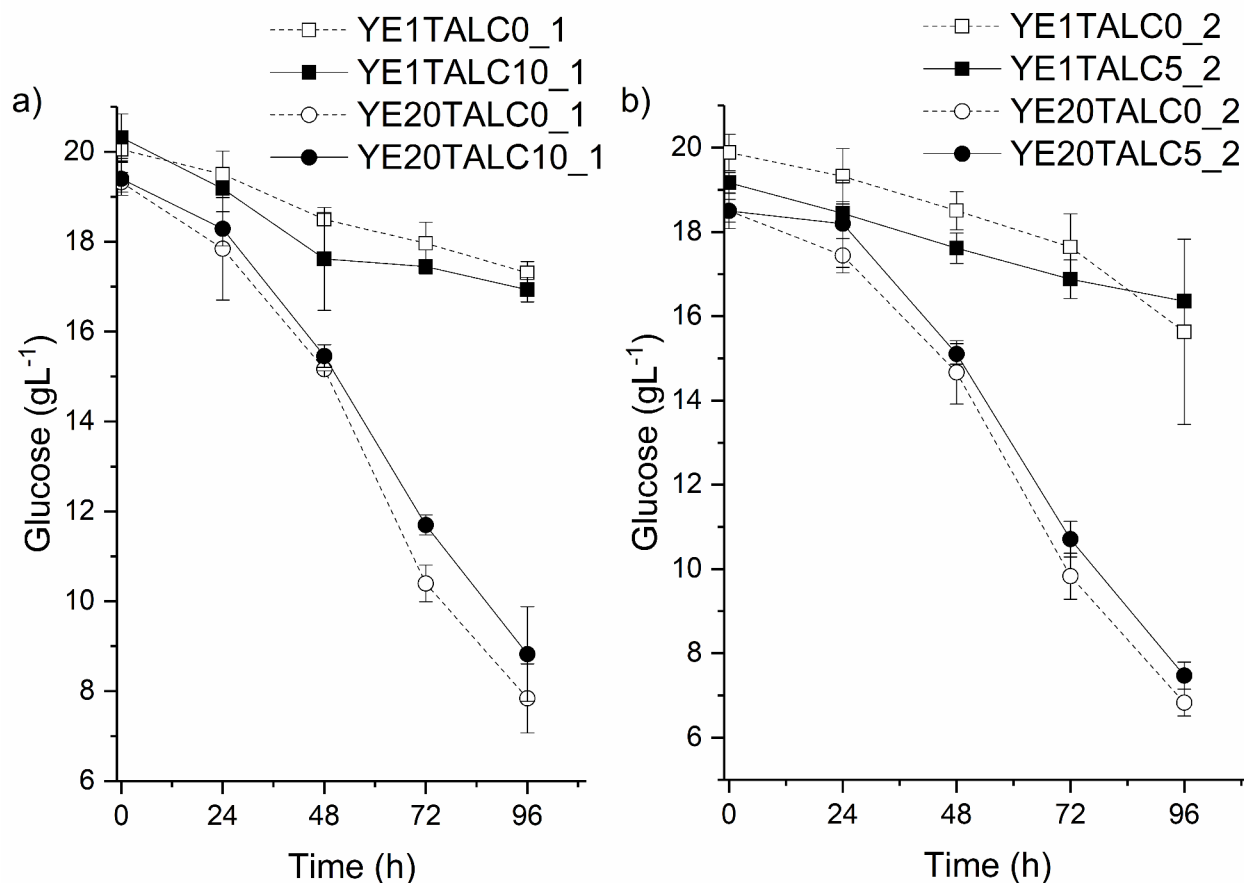


Fig. 6 Profiles of glucose utilization by *S. rimosus*

of nutritional substances in bioreactors and drew the same conclusions. They additionally measured pH levels in the cultures conducted in the medium containing 20 g L⁻¹ yeast extract. In those experiments, pH value decreased from the initial 6.25 below 5, while in the *S. rimosus* cultivations in the medium containing 1 and 5 g YE L⁻¹ pH slightly increased, up to 6.75. As pH value impacts filamentous microorganism morphology, especially the agglomeration of mycelial objects, and its lower levels promote the formation of dispersed forms, pH differences between the culture variants are an important insight [31].

Comparing cultivations without and with talc addition, in the *S. rimosus* MPEC runs talc microparticles embedded into pellets and caused the decrease in their sizes (Figs. 1 and 3). However, the final morphological forms in runs with 10 g TALC L⁻¹ differed with regard to size and shape when *S. rimosus* developed in the media containing low (1 g YE L⁻¹) and high (20 g YE L⁻¹) amount of nitrogen (Figs. 1 and 3). Furthermore, the class of non-agglomerates appeared only in the runs with high level of organic nitrogen (20 g YE L⁻¹). In the runs with 1 g YE L⁻¹ most of the pseudohyphae agglomerated, forming pellets.

The same morphological results on MPEC were obtained in the runs of the experiments conducted when half of the talc concentration was used (5 g TALC L⁻¹ instead of 10 g TALC L⁻¹). However, as it can be expected, the lower amount of talc caused the weaker effect on *S. rimosus* morphology. Nevertheless, a weaker morphological effect did not necessarily mean the aggravation of the production of secondary metabolites. Considering the conducted *S. rimosus* cultivations, the highest EFs for 2-methylthio-cis-zeatin (Fig. 5c) were obtained in the case when to the nitrogen-rich medium (20 g YE L⁻¹) 10 g TALC L⁻¹ of talc was added, and in the nitrogen-limited medium (1 g YE L⁻¹) only 5 g TALC L⁻¹ was used. It shows that when various media are used, the optimum talc concentration should be adjusted to the biosynthesis of the particular secondary metabolite. The topic of the selection of the appropriate microparticle material, its size and amount was raised for each new MPEC process [32]. However, the change in the action of microparticles dependent on the substrate requires further research.

In this work the addition of 5 and 10 g of talc microparticles was used. However, the range of the microparticles concentration applied in MPEC starts from 0.5 g L⁻¹. This

value was reported as optimal in UDP-glucose pyrophosphorylase bioproduction by *Grifola frondosa*. Talc microparticles addition assured the enhancement factor of the studied bioproduct at the level of 1.2 [33]. Nonetheless, the most often used microparticle concentrations range from 10 to 15 g L⁻¹. The examples are *Aspergillus ficuum* cultivations with talc microparticles for phytase production [34, 35] or *Rhizopus oryzae* biosynthesis of lactic acid enhanced by aluminium oxide addition [36]. High enhancement factor EF equal to 10 was obtained in MPEC of *Caldariomyces fumago* in chloroperoxidase bioproduction with talc addition of 10 g L⁻¹ [37]. The highest microparticles concentrations, up to 25 g L⁻¹ are found in MPEC supplemented by titanate microparticles. Here in an *Aspergillus niger* culture Driouch et al. [28] obtained enhanced factor EF for glucoamylase equal to 9.5. Nevertheless, it must be clearly stated that all these examples above deal with filamentous fungi and seeking the optimum amount of microparticles for this group of microorganisms. Unfortunately, there is a shortage of such data for actinomycetes [17, 18, 38].

Based on the conducted research, in the particular case of *S. rimosus* cultures the higher talc concentration (10 g TALC L⁻¹) was usually more efficient to enhance metabolite production than its lower amount (5 g TALC L⁻¹). This is consistent with the morphological impact (more significant for 10 g TALC L⁻¹) and shows the synergy between the microparticle effect on morphology and metabolism. Oxytetracycline production was enhanced only at the low initial nitrogen concentration and the decrease of talc concentration from 10 g TALC L⁻¹ to 5 g TALC L⁻¹ led to the ceasing of its production (Fig. 5a). What is more, *S. rimosus* did not produce oxytetracycline in the medium with 20 g YE L⁻¹ at all (with and without talc). Abou-Zeid et al. [27] stated that decreasing of nitrogen source is the way to promoting oxytetracycline production. Bizukojć et al. [30] associated inhibited production of this compound in the medium containing 20 g YE L⁻¹ with the decrease in pH that occurred in their experiments. As ADOTC is of polyketide origin and similar to oxytetracycline, its biosynthesis also took place in the medium containing low amount of nitrogen source, that is 1 g YE L⁻¹. In addition to the factors mentioned above, pseudohyphal morphology can also influence the synthesis of oxytetracycline and ADOTC. It varied significantly depending on the nitrogen concentration used (Fig. 1). In the media with 1 g YE L⁻¹ regular pellets developed, whilst in the runs conducted using 20 g L⁻¹ yeast extract small, irregular agglomerates and dispersed hyphae prevailed.

The example of enhancement factors for lorneic acid J and milbemycin A₃ in the conducted *S. rimosus* cultivations showed that the final effect of MPEC was strictly connected with nitrogen content. This is why

the medium should be selected on the basis of the structure and metabolic pathway of the compound. A 10 g TALC L⁻¹ addition in the medium containing 1 g YE L⁻¹ improved lorneic acid J production, whilst in the medium with 20 g YE L⁻¹ the effect of talc addition was opposite and EF decreased below 1 (Fig. 5d). Similar to lorneic acid J, nitrogen content in the culture medium influenced milbemycin A₃ enhancement factor EF. Importantly, for milbemycin A₃ the value of EF equal to 1.2 was observed in MPEC at 20 g YE L⁻¹ whereas it was only 0.8 in 96 h at 1 g YE L⁻¹. The analysis of spinoxazine A and two unidentified compounds with experimental m/z value [M-H]⁻ ion: m/z=608.2843 and m/z=595.6595 (Fig. 5f, g and h) confirmed again the well-known statement that the culture medium composition influences filamentous microorganisms metabolism. These three compounds occurred only in *S. rimosus* cultivations conducted in the medium containing 20 g YE L⁻¹. The deficiency of nitrogen source in the runs of the experiments with yeast extract 1 g L⁻¹ did not promote their biosynthesis, both in control runs without microparticles and MPEC. Therefore, it can be concluded that the first step in the effective designing MPEC for the filamentous microorganisms is the selection of the appropriate medium and next of microparticles and their concentration. Statistical methods like Plackett–Burman design (PBD) combined with Response Surface Methodology (RSM) might prove to be a suitable tool [4, 6] for future studies on MPEC.

All in all, this work delivered the number of crucial information on the improvement of *S. rimosus* cultivations, a graphical summary of which is presented in Fig. 7.

Increasing the nitrogen concentration in the cultivation medium resulted in the formation of smaller agglomerates (Fig. 7) and promoted the biosynthesis of one of *S. rimosus* metabolites namely spinoxazine A. Secondary metabolites of polyketide origin like oxytetracycline were produced only at the low initial nitrogen source concentration. However, this culture medium promoted the development of large pellets which are known to be inefficient in the biosynthesis processes mainly due to limitation in the transfer of substrates. Thus in order to increase metabolite production without changing the composition of the culture medium, the addition of microparticles was used. The presence of the microparticles in the cultivation medium caused the development of dispersed pseudomycelium and smaller pellets, and possibly led to the improvement of nutrient and oxygen diffusion to the interior of the agglomerates. Increasing concentration of talc microparticles showed a stronger influence on *S. rimosus* morphology as the smaller morphological objects then appeared in the MPEC. Therefore, for those secondary metabolites, whose biosynthesis is to the high extent connected with the morphology of

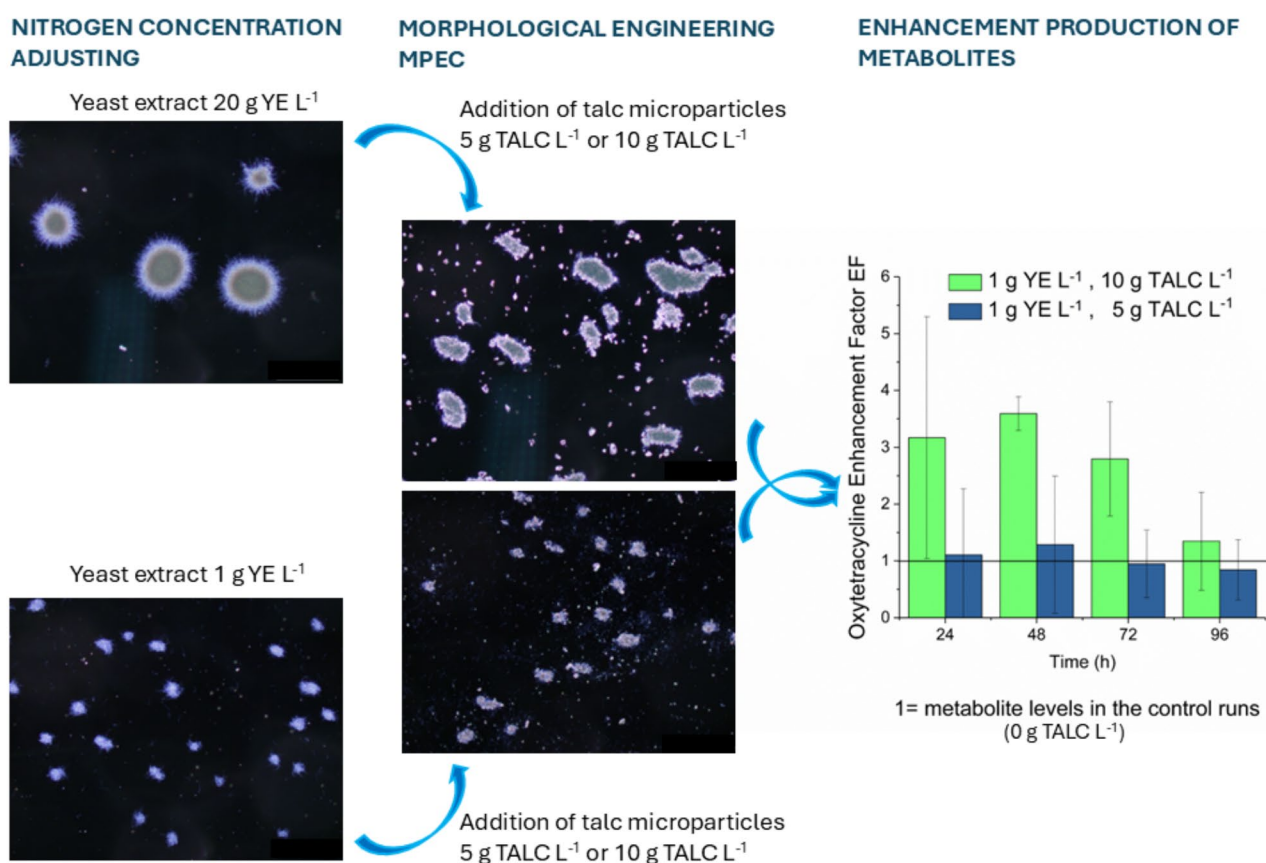


Fig. 7 Graphical summary of the results

the microorganism, as oxytetracycline or ADOTC, the increase of the Enhancement Factor depended on the talc concentration. On the other hand, 2-methylthio-cis-zeatin was an example of a metabolite for which the correlations between morphology, culture medium composition and talc concentration were not so clear if any existed.

Conclusions

On the basis of the performed experiments several findings can be drawn.

Microparticle-enhanced cultivations of *S. rimosus* conducted in the same process conditions lead to different morphological forms of the actinomycetes dependent on the amount of nitrogen in the medium.

The low nitrogen content in the medium leads to the limitation of *S. rimosus* growth and, in consequence, the development of the lower number of larger agglomerates than in the culture containing the high amount of nitrogen source. The high concentration of yeast extract promotes the development of small agglomerates and dispersed hyphae of *S. rimosus*.

Talc microparticles embedded into such agglomerates as pellets decrease their size. However, the power of the

effect of microparticles on *S. rimosus* morphology and main metabolite production depends on the amount of microparticles added to the medium. The synergy between the microparticle effect on morphology and metabolism of *S. rimosus* is especially noticeable in the biosynthesis of oxytetracycline, ADOTC and spinoxazine A leading to the respective 4-,5- and 1.6-fold increase of their production.

In the case of 2-methylthio-cis-zeatin, a weaker effect of microparticles on *S. rimosus* morphology does not necessarily aggravate the biosynthesis of this metabolite so ultimately the optimum talc concentration should be adjusted to the biosynthesis of the particular secondary metabolite in conjunction with the selection of the medium composition.

Supplementary Information

The online version contains supplementary material available at <https://doi.org/10.1186/s12934-024-02514-x>.

Supplementary Material 1

Acknowledgements

This work was financed by the National Science Centre (Republic of Poland); grant number 2021/43/B/ST8/00268.

Author contributions

AS: Conceptualization, Methodology, Investigation, Formal analysis, Writing-Original draft preparation. TB: Conceptualization, Methodology, Investigation, Formal analysis, Writing - Review and Editing. WG: Investigation. MB: Resources, Investigation, Writing - Review and Editing, Supervision, Project administration. All authors read and approved the final manuscript.

Data availability

No datasets were generated or analysed during the current study.

Declarations

Ethics approval and consent to participate

Not applicable.

Consent for publication

Not applicable.

Competing interests

The authors declare no competing interests.

Received: 1 July 2024 / Accepted: 24 August 2024

Published online: 09 September 2024

References

- Pommerehne K, Walisch J, Ebersbach A, Krull R. The antitumor antibiotic rebeccamycin - challenges and advanced approaches in production processes. *Appl Microbiol Biotechnol*. 2019;103:3627–36. <https://doi.org/10.1007/s00253-019-09741-y>
- Del Carratore F, Hanko EK, Breitling R, Takano E. Biotechnological application of *Streptomyces* for the production of clinical drugs and other bioactive molecules. *Curr Opin Biotechnol*. 2022;77:102762. <https://doi.org/10.1016/j.copbio.2022.102762>
- Bode HB, Bethe B, Höfs R, Zecek A. Big effects from small changes: possible ways to explore nature's chemical diversity. *Chem Bio Chem*. 2002;3:619–27. [https://doi.org/10.1002/1439-7633\(20020703\)3:7<619::AID-CBIC619>3.0.CO;2-9](https://doi.org/10.1002/1439-7633(20020703)3:7<619::AID-CBIC619>3.0.CO;2-9)
- Zhang D, Bao Y, Ma Z, Zhou J, Chen H, Lu Y, Chen LZ, Chen X. Optimization of fermentation medium and conditions for enhancing valinomycin production by *Streptomyces* sp. ZJUT-IFE-354. *Prep. Biochem Biotechnol*. 2023;53:157–66. <https://doi.org/10.1080/10826068.2022.2053991>
- Saleena SK, Johnson JJ, Joseph JK, Padinchaty KK, Abdulla MHA. Production and optimization of L-asparaginase by *Streptomyces koyangensis* SK4 isolated from Arctic sediment. *J Basic Microbiol*. 2023;63:417–26. <https://doi.org/10.1002/jobm.202200116>
- Abdella B, Abdella M, ElSharif HA, ElAhwany AMD, El Sersy NA, Ghozlan HA, Sabry SA. Identification of potent anti-candida metabolites produced by the soft coral associated *Streptomyces* sp. HC14 using chemoinformatics. *Sci Rep*. 2023;13:12564. <https://doi.org/10.1038/s41598-023-39568-7>
- He Z, Sun Y, Chu M, Zhu J, Zhang Y, Tang Q, Osman G, Jiang L, Zhang Z. Screening of a novel fibrinolytic enzyme-producing *Streptomyces* from a hyper-arid area and optimization of its fibrinolytic enzyme production. *Ferment*. 2023;9:410. <https://doi.org/10.3390/fermentation9050410>
- Preethi PS, Vickram AS, Das R, Hariharan NM, Rameshpathy M, Subbaiya R, Karmegam N, Kim W, Govarthanan M. Bioprospecting of novel peroxidase from *Streptomyces coelicolor* strain SPR7 for carcinogenic azo dyes decolorization. *Chemosphere*. 2023;310:136836. <https://doi.org/10.1016/j.chemosphere.2022.136836>
- Alloun W, Berkani M, Benaissa A, Shavandi A, Gares M, Danesh C, Lakhdari D, Ghfar AA, Chaouche NK. Waste valorization as low-cost media engineering for auxin production from the newly isolated *Streptomyces rubrogriseus* AW22: Model development. *Chemosphere*. 2023;326:138394. <https://doi.org/10.1016/j.chemosphere.2023.138394>
- Rigali S, Titgemeyer F, Barends S, Mulder S, Thomae AW, Hopwood DA, van Wezel GP. Feast or famine: the global regulator DasR links nutrient stress to antibiotic production by *Streptomyces*. *EMBO Rep*. 2008;9:670–5. <https://doi.org/10.1038/embor.2008.83>
- van Wezel GP, Krabben P, Traag BA, Keijsers BJF, Kerste R, Vijgenboom E, Heijnen JJ, Kraal B. Unlocking *Streptomyces* spp. for use as sustainable industrial production platforms by morphological engineering. *Appl Environ Microbiol*. 2006;72:5283–8. <https://doi.org/10.1128/AEM.00808-06>
- Veiter L, Rajamanickam V, Herwig C. The filamentous fungal pellet—relationship between morphology and productivity. *Appl Microbiol Biotechnol*. 2018;102:2997–3006. <https://doi.org/10.1007/s00253-018-8818-7>
- Jonsbu E, McIntyre M, Nielsen J. The influence of carbon sources and morphology on nystatin production by *Streptomyces noursei*. *J Biotechnol*. 2002;95:133–44. [https://doi.org/10.1016/S0168-1656\(02\)00003-2](https://doi.org/10.1016/S0168-1656(02)00003-2)
- Anteck A, Bizukojc M, Ledakowicz S. Modern morphological engineering techniques for improving productivity of filamentous fungi in submerged cultures. *World J Microbiol Biotechnol*. 2016;32:193. <https://doi.org/10.1007/s11274-016-2148-7>
- Holtmann D, Verner F, Müller JM, Kaden D, Risse JM, Friehs K, Dähne L, Strattmann A, Schrader J. Effects of particle addition to *Streptomyces* cultivations to optimize the production of actinorhodin and streptavidin. *Sustain Chem Pharm*. 2017;5:67–71. <https://doi.org/10.1016/j.scp.2016.09.001>
- Karahalil E, Coban HB, Turhan I. A current approach to the control of filamentous fungal growth in media: microparticle enhanced cultivation technique. *Crit Rev Biotechnol*. 2018;39:192–201. <https://doi.org/10.1080/07388551.2018.1531821>
- Kuhl M, Rückert C, Gläser L, Beganovic S, Luzhetskyy A, Kalinowski J, Wittmann C. Microparticles enhance the formation of seven major classes of natural products in native and metabolically engineered actinobacteria through accelerated morphological development. *Biotechnol Bioeng*. 2021;118:3076–93. <https://doi.org/10.1002/bit.27818>
- Kuhl M, Gläser L, Rebets Y, Rückert C, Sarkar N, Hartsch T, Kalinowski J, Luzhetskyy A, Wittmann C. Microparticles globally reprogram *Streptomyces albus* toward accelerated morphogenesis, streamlined carbon core metabolism, and enhanced production of the antituberculosis polyketide pamamycin. *Biotechnol Bioeng*. 2020;117:3858–75. <https://doi.org/10.1002/bit.27537>
- Böl M, Schrinner K, Tesche S, Krull R. Challenges of influencing cellular morphology by morphology engineering techniques and mechanical induced stress on filamentous pellet systems - A critical review. *Eng Life Sci*. 2020;21:51–67. <https://doi.org/10.1002/elsc.202000060>
- Kumar P, Khushboo R, Dt, Dubey KK. Insights into the mechanism of mycelium transformation of *Streptomyces toxytricini* into pellet. *FEMS Microb*. 2023;4:xtad017. <https://doi.org/10.1093/femsmc/xtad017>
- Kowalska A, Boruta T, Bizukojc M. Morphological evolution of various fungal species in the presence and absence of aluminum oxide microparticles: comparative and quantitative insights into microparticle-enhanced cultivation (MPEC). *Microb. Open*. 2018;7:e603. <https://doi.org/10.1002/mbo3.603>
- Yue C, Xu H, Yu Y, Yu X, Yu M, Zhang C, You Q, Xia S, Ding Z, Fu H, Zeng X, Li F. Improvement of natamycin production by controlling the morphology of *Streptomyces Gilvosporeus* Z8 with microparticle talc in seed preculture. *JCTB*. 2021;96:1533–42. <https://doi.org/10.1002/jctb.6668>
- Khushboo DN, Kashyap Dubey KK. Effect of natural precursors and micro/macroparticles addition on the morphology modulation of *Streptomyces toxytricini* KD18 stimulates lipstatin productivity. *bioRxiv*. 2023. <https://doi.org/10.1101/2023.07.02.547449>. In press.
- Wucherpennig T, Hestler T, Krull R. Morphology engineering – osmolality and its effect on *Aspergillus Niger* morphology and productivity. *Microb Cell Fact*. 2011;10:58. <https://doi.org/10.1186/1475-2859-10-58>
- Kowalska A, Boruta T, Bizukojc M. Performance of fungal microparticle-enhanced cultivations in stirred tank bioreactors depends on species and number of process stages. *Biochem Eng J*. 2020;161:107696. <https://doi.org/10.1016/j.bej.2020.107696>
- Boruta T, Ścigaczewska A, Bizukojc M. Microbial Wars in a stirred Tank Bioreactor: investigating the co-cultures of *Streptomyces rimosus* and *Aspergillus Terreus*, filamentous microorganisms equipped with a Rich Arsenal of secondary metabolites. *Front Bioeng Biotechnol*. 2021;9:713639. <https://doi.org/10.3389/fbioe.2021.713639>
- Abou-Zeid AA, El-Diwanly AI, Shaker HM, Salem HM. Role of nitrogen sources in fermentative production of oxytetracycline by *Streptomyces rimosus* 93060. *Agric. Wastes*. 1981;3:57–265. [https://doi.org/10.1016/0141-4607\(81\)90012-3](https://doi.org/10.1016/0141-4607(81)90012-3)
- Drriouch H, Hänsch R, Wucherpennig T, Krull R, Wittmann C. Improved enzyme production by bio-pellets of *Aspergillus Niger*: targeted morphology engineering using titanate microparticles. *Biotechnol Bioeng*. 2012;109:462–71. <https://doi.org/10.1002/bit.23313>
- Bizukojc M, Ledakowicz S. The morphological and physiological evolution of *aspergillus terreus* mycelium in the submerged culture and its relation to the formation of secondary metabolites. *World J Microbiol Biotechnol*. 2010;26:41–54. <https://doi.org/10.1007/s11274-009-0140-1>

30. Bizukojć M, Ścigaczewska A, Boruta T, ruda A, Kawka A. Bioreactor study of the metabolic repertoire and morphology of actinomycete *Streptomyces rimosus* ATCC 10970 under various initial concentrations of carbon and nitrogen sources, *Chem. Process Eng. New. Front.* In press. <https://doi.org/10.24425/cpe.2023.147414>
31. Papagianni M. Fungal morphology and metabolite production in submerged mycelial processes, *Biotechnol. Adv.* 2004;22:189–259. <https://doi.org/10.1016/j.biotechadv.2003.09.005>
32. Liable AR, Dinius A, Schrader M, Krull R, Kwade A, Briesen H, Schmideder S. Effects and interactions of metal oxides in microparticle-enhanced cultivation of filamentous microorganisms. *Eng Life Sci.* 2022;709–817. <https://doi.org/10.1002/elsc.202100075>
33. Tao TL, Cui FJ, Chen XX, Sun WJ, Huang DM, Zhang J, Yang Y, Wu D, Liu WM. Improved mycelia and polysaccharide production of *Grifola frondosa* by controlling morphology with microparticle talc, *Microb. Cell Fact.* 2018;17:1. <https://doi.org/10.1186/s12934-017-0850-2>
34. Coban HB, Demirci A, Turhan I. Microparticle-enhanced *aspergillus ficuum* phytase production and evaluation of fungal morphology in submerged fermentation. *Bioprocess Biosyst Eng.* 2015;38:1075–80. <https://doi.org/10.1007/s00449-014-1349-4>
35. Coban HB, Demirci A, Turhan I. Enhanced *aspergillus ficuum* phytase production in fed-batch and continuous fermentations in the presence of talcum microparticles. *Bioprocess Biosyst Eng.* 2015;38:1431–6. <https://doi.org/10.1007/s00449-015-1384-9>
36. Coban HB, Demirci A. Enhancement and modeling of microparticle-added *Rhizopus oryzae* lactic acid production. *Bioprocess Biosyst Eng.* 2016;39:323–30. <https://doi.org/10.1007/s00449-015-1518-0>
37. Kaup BA, Ehrich K, Pescheck M, Schrader J. Microparticle-enhanced cultivation of filamentous microorganisms: increased chloroperoxidase formation by *Caldariomyces Fumago* as an example. *Biotechnol Bioeng.* 2008;99:491–8. <https://doi.org/10.1002/bit.21713>
38. Boruta T, Anteck A. Co-cultivation of filamentous microorganisms in the presence of aluminum oxide microparticles. *Appl Microbiol Biotechnol.* 2022;106:5459–77. <https://doi.org/10.1007/s00253-022-12087-7>

Publisher's note

Springer Nature remains neutral with regard to jurisdictional claims in published maps and institutional affiliations.